



## Using metadynamics to explore complex free-energy landscapes

Giovanni Bussi<sup>1</sup> and Alessandro Laio<sup>1,2</sup>

**Abstract** | Metadynamics is an atomistic simulation technique that allows, within the same framework, acceleration of rare events and estimation of the free energy of complex molecular systems. It is based on iteratively ‘filling’ the potential energy of the system by a sum of Gaussians centred along the trajectory followed by a suitably chosen set of collective variables (CVs), thereby forcing the system to migrate from one minimum to the next. The power of metadynamics is demonstrated by the large number of extensions and variants that have been developed. The first scope of this Technical Review is to present a critical comparison of these variants, discussing their advantages and disadvantages. The effectiveness of metadynamics, and that of the numerous alternative methods, is strongly influenced by the choice of the CVs. If an important variable is neglected, the resulting estimate of the free energy is unreliable, and predicted transition mechanisms may be qualitatively wrong. The second scope of this Technical Review is to discuss how the CVs should be selected, how to verify whether the chosen CVs are sufficient or redundant, and how to iteratively improve the CVs using machine learning approaches.

Metastability is characteristic of many interesting systems in materials science and biophysics. Technically speaking, metastability arises when the probability distribution as a function of the atomic coordinates has at least two peaks (the metastable states) separated by a region in which the probability is many orders of magnitude lower. The prototypical example of this situation is a molecule that can undergo a chemical reaction: the two probability peaks correspond to the reactant and the product states. Other secondary probability peaks, if present, correspond to the intermediate states of the reaction. In practical terms, metastability means that a molecular dynamics (MD) or a Monte Carlo (MC) simulation is likely to remain stuck in only one probability maximum (typically corresponding to an energy minimum) for the duration of the run. Since the early days of molecular simulations, researchers have attempted to develop approaches to fight this problem, with the goal of observing all the relevant metastable states in the limited time that can be afforded in a simulation.

A possible route to this goal involves ‘filling’ the free-energy minima of the metastable states in a controlled way and thereby enabling the system to explore all states. To do so requires first choosing, on the basis of chemical or physical intuition, a low-dimensional collective variable (CV), namely, a function of the coordinates that takes a different value in all the relevant metastable

states. For example, in a chemical reaction in which a specific bond in a molecule should break, an appropriate CV would be the distance between the two atoms forming the bond. We denote the CV by  $S(x)$ , where  $x$  denotes the coordinates of the system (such as positions of all atoms). Given a CV, the probability distribution  $P(x)$  can be reduced to a function of the CV by integrating  $P(x)$  over all  $x$  under the constraint  $S(x) = s$ :

$$P(s) = \int dx P(x) \delta(s - S(x)) \quad (1)$$

In this discussion, we assume that  $P(x)$  is the canonical distribution associated with a potential energy function  $V(x)$ :  $P(x) \propto \exp(-V(x)/T)$ , where  $T$  is the temperature (to simplify notation, we use units in which the Boltzmann constant is one). If the CV is well chosen, the metastable states appear as separate and well-defined peaks in  $P(s)$ . The free energy as a function of  $s$  is

$$F(s) = -T \log(P(s)) \quad (2)$$

Correspondingly, for a system with metastable states, the free energy as a function of a good CV has (at least) two well-defined minima.

If one is fortunate, for the molecular system under study both a good CV and an approximation  $B(s)$  of the negative of the free energy are known. In that case, the metastability problem in that system can be considered

<sup>1</sup>SISSA, Trieste, Italy.

<sup>2</sup>ICTP, Trieste, Italy.

e-mail: laio@sissa.it

<https://doi.org/10.1038/s42254-020-0153-0>

## Key points

- Metadynamics makes it possible to accelerate conformational transitions between metastable states, broadening the scope of molecular dynamics simulations.
- Like other enhanced sampling methods, metadynamics requires the introduction of low-dimensional descriptors (collective variables) whose choice affects the rate at which transitions are enhanced. The ideal collective variable should take different values not only in all the relevant metastable states but also in the transition states between them.
- The appropriate collective variables can be found by trial and error or designed automatically using methods inspired by machine learning.
- Two variants of metadynamics are commonly used, namely ordinary and well-tempered metadynamics. The former has the advantage of inducing transitions between the metastable states even if the collective variable is not ideal. The latter has the advantage of providing an exact estimator of the free energy.
- Metadynamics can be used in combination with most molecular dynamics software packages by taking advantage of dedicated software libraries that implement the method and a large number of collective variables.

as solved. This is because MD or MC simulations can be run with a modified potential  $\tilde{V}(x) = V(x) + B(S(x))$ . The probability distribution as a function of the CV becomes

$$\begin{aligned} \tilde{P}(s) &= C \int dx e^{-\frac{V(x)+B(S(x))}{T}} \delta(s - S(x)) \\ &= C' e^{-\frac{F(s)+B(s)}{T}} \end{aligned} \quad (3)$$

where  $C$  and  $C'$  are normalization constants. Therefore, if  $B(s) \approx -F(s)$ , the probability distribution as a function of  $s$  is approximately flat. The simulation is no longer confined in a metastable state and can freely diffuse across the barrier. Although the simulation is performed under the action of a potential that is modified by an external bias, it is straightforward to estimate the unbiased free energy from the biased probability distribution of  $s$ , because taking the logarithm of both sides of equation 3 gives  $F(s) = -B(s) - T \log(\tilde{P}(s)) + C$ , where  $C$  is a constant.

This 'trick' has been well known since the early days of molecular simulations<sup>1</sup>, but its practical applicability is hindered by three problems:

- Before performing the simulation, what the free energy looks like is unknown, and a good choice for  $B(s)$  is in general unavailable.
- In many cases, finding a good CV is non-trivial. It is possible to build, based on intuition, a CV capable of distinguishing the metastable states, but this variable is not necessarily good for describing the transition, as we discuss.
- In other cases, even the relevant metastable states are unknown. For example, one may wish to study the conformational transition of a complex biomolecule, knowing only the structure of the molecule in one state. This situation is possibly the most relevant for practical applications.

Metadynamics<sup>2</sup> is an algorithm that can satisfactorily solve the first problem by building  $B$  in an iterative process. However, it does not provide a CV even if, as we discuss, it enables verification that a CV is good

and improvement of the CV for a successive simulation. Moreover, and possibly most importantly, metadynamics allows simultaneous use of multiple CVs. This, as we discuss, makes it possible to be less picky in the choice of the CVs and, in some special cases, even address the problem of unknown metastable states.

Several reviews discussing the theory of metadynamics and its applications in a number of different fields are available<sup>3–8</sup>. We give a brief introduction to metadynamics, but this Technical Review is primarily focused on the technical decisions that must be made before performing a metadynamics simulation. In particular, we discuss the advantages and disadvantages of the different variants of this approach, the proper assessment of errors, the detection of critical cases where metadynamics is difficult to apply, the recently introduced methods to determine CVs using machine learning techniques and the available implementations of the method.

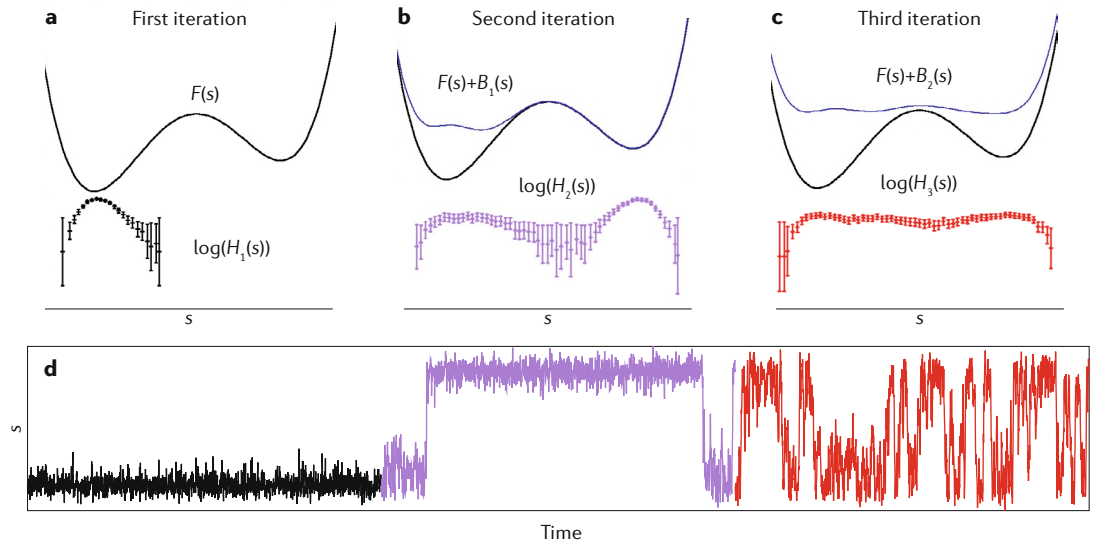
## Introduction to metadynamics

Metadynamics was originally developed in the spirit of time-stepper-based approaches<sup>9</sup>. Metadynamics embedded two ideas in that framework: filling the free-energy minima, similar to what was proposed in REF.<sup>10</sup>, and biasing the dynamics by a history-dependent potential, as was previously done in taboo search<sup>11,12</sup>, local elevation<sup>13</sup> and Wang–Landau sampling<sup>14</sup>. However, to understand more clearly the working principle of metadynamics, it is convenient to heuristically introduce it as a limiting case of adaptive umbrella sampling (AUS)<sup>15</sup>, which is another method for constructing a bias potential. AUS requires running a sequence of relatively short simulations, here labelled by an index  $r$ . Each simulation is biased by a different external potential  $B_r(s)$ , built iteratively (FIG. 1a–d) by: running a simulation under the action of the potential  $V(x) + B_r(S(x))$ ; computing the histogram  $H_r(s)$  of the CV, with the first part of the simulation discarded, to allow an appropriate equilibration; updating the bias:

$$B_{r+1}(s) = B_r(s) + T \log(H_r(s)) \quad (4)$$

In practice, to use  $B_r$  as an external bias in an MD simulation, it is important to represent the logarithm of the histogram by a smooth function, for example, a spline. A drawback of AUS is that approximating this function can be non-trivial, because the histogram is affected by non-uniform errors. Initially, the bias is zero. Because the simulation is short, the system remains stuck in the first metastable state. The histogram  $H_1(s)$  spans only that minimum. The key idea of AUS is that the logarithm of this histogram is an estimate of the free energy, restricted to the region that has been explored so far. In other words,  $F(s) + T \log(H_r(s))$  is approximately constant in the region of the minimum. In the second run, the system, owing to the effect of the bias, explores a wider range of the CV, performing a transition to the second minimum. The new histogram is approximately flat in the region already explored in the first run, and it provides information on the shape of the free energy on a wider range. In the example in (FIG. 1), the bias potential has already 'filled' the free-energy landscape after three iterations. At this point,  $B_r(s) \approx -F(s)$ .

## Adaptive umbrella sampling



## Metadynamics

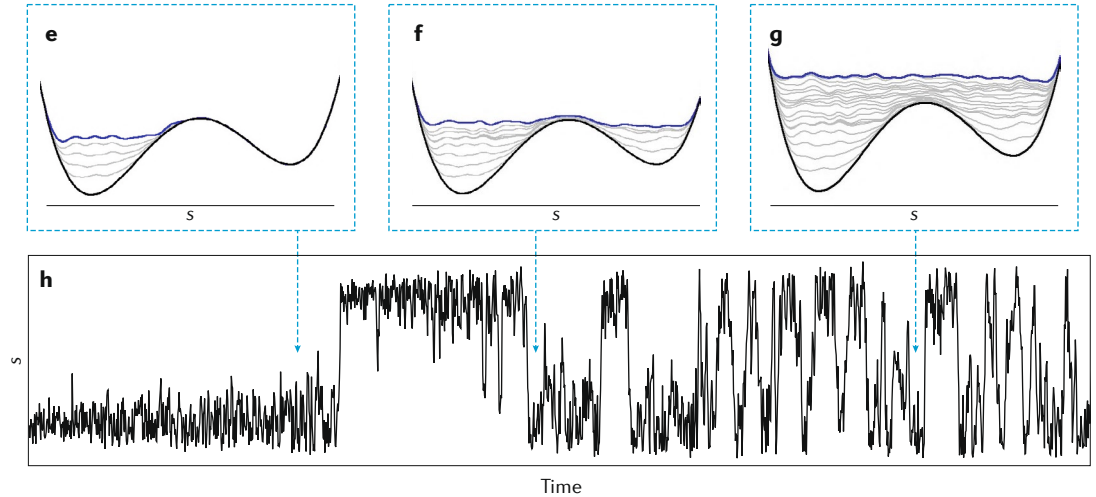


Fig. 1 | **The working principles of adaptive umbrella sampling and metadynamics.** **a–c** | The first (panel **a**), second (panel **b**) and third (panel **c**) iterations of adaptive umbrella sampling. The black curve, identical in the three panels, is the free energy that has to be reconstructed. The purple curve in panels **b** and **c** is the sum of the free energy and of the bias in the second iteration (panel **b**) and third iteration (panel **c**). The points with error bars at the bottom of the panels represent the histogram  $H$  of the collective variable (CV)  $s$  estimated in each iteration. **d** | The CV  $s$  as a function of time in the three iterations. **e–g** | The sum of the free energy and of the metadynamics bias potential (equation 7; blue lines) at three different times marked by arrows in panel **h**, along with the free energy (black lines). **h** | The CV  $s$  as a function of time in a metadynamics simulation.

Metadynamics can be viewed as a limiting case of AUS. Imagine making the simulation time between updates of the bias so short that the value of the CV does not change notably during the run. In this case, the label  $r$  designating the different runs in AUS can be replaced by a label  $t$ , labelling simulation time. The histogram  $H_t(s)$  becomes a single peak, localized in the close neighbourhood of  $s_t = S(x_t)$ . The key idea of metadynamics is to approximate the logarithm of this histogram with a simple, differentiable function. Typically, a Gaussian of width  $\sigma$  and height  $w$  is used:

$$T \log(H_t(s)) \sim w \exp\left(-\frac{(s_t - s)^2}{2\sigma^2}\right) \quad (5)$$

This turns equation 4 into

$$B_{t+1}(s) = B_t(s) + w \exp\left(-\frac{(s_t - s)^2}{2\sigma^2}\right) \quad (6)$$

or, equivalently

$$B_t(s) = w \sum_{t' < t} \exp\left(-\frac{(s_{t'} - s)^2}{2\sigma^2}\right) \quad (7)$$

Initially, the Gaussians are all localized in the first free-energy minimum (FIG. 1e–h). These Gaussians induce larger and larger fluctuations in the CV (FIG. 1h). After some time, the first free-energy minimum is almost

completely filled by Gaussians (FIG. 1e) and the system performs a transition to the second minimum. This second minimum is also filled with Gaussians (FIG. 1f). After that moment, the CV starts diffusing freely between the two minima (FIG. 1h). The sum of the Gaussians now compensates almost exactly the free energy (FIG. 1g). This sum can be therefore used to estimate  $F(s)$ . The two parameters  $w$  and  $\sigma$  can be tuned to control the speed at which the free-energy landscape is filled and, thus, flattened. If larger Gaussians are used, the bias will grow quickly, but the system will be strongly out of equilibrium. If, instead, the Gaussians are small, metadynamics becomes a quasi-equilibrium process, very similar to AUS. The precise role of these parameters is discussed below.

Replacing the logarithm of the histogram in equation 4 with a Gaussian in equation 6 can be viewed as a convenient way to smooth the former, in a spirit similar to kernel density estimators<sup>16</sup>. For example, to compute the free energy as a simultaneous function of three different CVs, in AUS it is first necessary to compute a histogram as a function of three coordinates, and then represent its logarithm by a regular and differentiable function. In metadynamics, the function is built as a sum of three-dimensional Gaussians localized along the trajectory followed by the system in CV space. As has been shown in many applications, and rigorously demonstrated for model dynamics, equation 7 provides a good approximation to the negative free energy in three dimensions or even more. The ability to compute the free energy as a function of multiple CVs is the most important practical advantage of metadynamics with respect to other methods.

The formulation of equation 7 makes it apparent that in metadynamics the coordinates of the system evolve under the action of a non-Markovian process, that is, the forces are history dependent: the dynamics at time  $t$  is biased by an external potential defined by a sum of Gaussians localized on the sequence of values taken by the CV up to that moment. Before the introduction of metadynamics, approaches such as local elevation<sup>13</sup> used the idea of enhancing sampling using Gaussians without attempting to estimate the free energy from the sampled states. The most important contribution of the work in which metadynamics was introduced<sup>2</sup> was to conjecture that the history-dependent potential in equation 7 can be used to estimate the free energy.

The non-Markovian nature of the dynamics makes its theoretical description more complex. However, by explicitly considering the external bias as a dynamic variable, the resulting dynamics is fully Markovian in an extended space, the coordinates  $x$  and the bias  $B(s)$  (REF.<sup>17</sup>). In these variables, the evolution of the system at time  $t$  depends only on its state at that time. When compared with the heuristic derivation above, the demonstration of REF.<sup>17</sup> makes the assumption of adiabatic separation between the biased CV and the other degrees of freedom of the system but allows for an exact demonstration that is valid also in the case of a finite Gaussian deposition rate. The existence of such an exact demonstration is the most important conceptual difference with respect to AUS. In this formulation, it becomes natural to treat the bias potential in the same way as an ordinary observable in a finite-temperature MD or MC run: its instantaneous

shape is not particularly meaningful, because it is affected by fluctuations. Instead, the relevant free-energy estimator is not the bias itself, but its time average, in which the fluctuations become progressively smaller. These topics are treated extensively in the next section.

Because the amplitude of the fluctuations in the bias potential is proportional to the height of the added Gaussian  $w$ , it is possible to reduce these fluctuations during the simulation by suitably reducing  $w$ . One possible way to do so is to employ well-tempered metadynamics<sup>18</sup>, in which the height of the Gaussians is chosen to be proportional to a decaying exponential function of the potential deposited in the currently visited point of the CV space. Then, equation 6 becomes

$$B_{t+1}(s) = B_t(s) + \exp\left(-\frac{B_t(s)}{\Delta T}\right) \exp\left(-\frac{(s_t - s)^2}{2\sigma^2}\right) \quad (8)$$

where  $\Delta T$  is a parameter that controls how quickly the Gaussian height is decreased. Often,  $\Delta T$  is written in terms of a so-called bias factor  $\gamma = \frac{T + \Delta T}{T}$ . It can be shown that in well-tempered metadynamics, the height of the Gaussian deposited at a given point decreases proportionally to the inverse of the time the simulation spent at that point<sup>18</sup>. This one-over-time relationship is commonly used for the learning rate in stochastic minimizations in machine learning approaches<sup>19</sup>, because it is guaranteed to converge<sup>20</sup>. However, by using a height that implicitly depends on the position in the CV space, in the long-time limit, the system does not sample a flat distribution. The bias potential does not converge to  $-F(s)$  but rather to a fraction of the free energy  $-\frac{\Delta T}{T + \Delta T}F(s)$  that is known a priori, and the system thus samples the distribution  $P \propto \exp\left(-\frac{F(s)}{(T + \Delta T)}\right)$ . Therefore,  $\Delta T$  has the role of both damping the fluctuations of the estimator and controlling the effective temperature at which the chosen CV is sampled. In non-well-tempered metadynamics, this effective temperature is infinite. The scheme can be further generalized to control the fluctuations of the estimator and the effective temperature of the CV independently<sup>20</sup>.

An important difference between well-tempered and non-well-tempered metadynamics relates to the state reached at long times. If boundary conditions are properly treated, non-well-tempered metadynamics is guaranteed to reach a stationary state in which the bias potential fluctuates. This stationary state is conditional on filling the relevant free-energy wells. Well-tempered metadynamics, instead, reaches a quasi-equilibrium state, in which the bias potential provides an exact estimator for the free energy<sup>18,20</sup>. Such a quasi-equilibrium state is guaranteed for only an infinitely long trajectory. It might thus be convenient to heuristically use the time average of the bias potential as a better estimator for the free-energy surface also in well-tempered metadynamics (as discussed in the next section).

## Choosing the CVs

The capability of metadynamics to accelerate rare-event sampling and to reconstruct free-energy landscapes crucially depends on the employed CVs (FIG. 2). This dependence is common to all methods based on adding a bias potential that only depends on selected CVs.

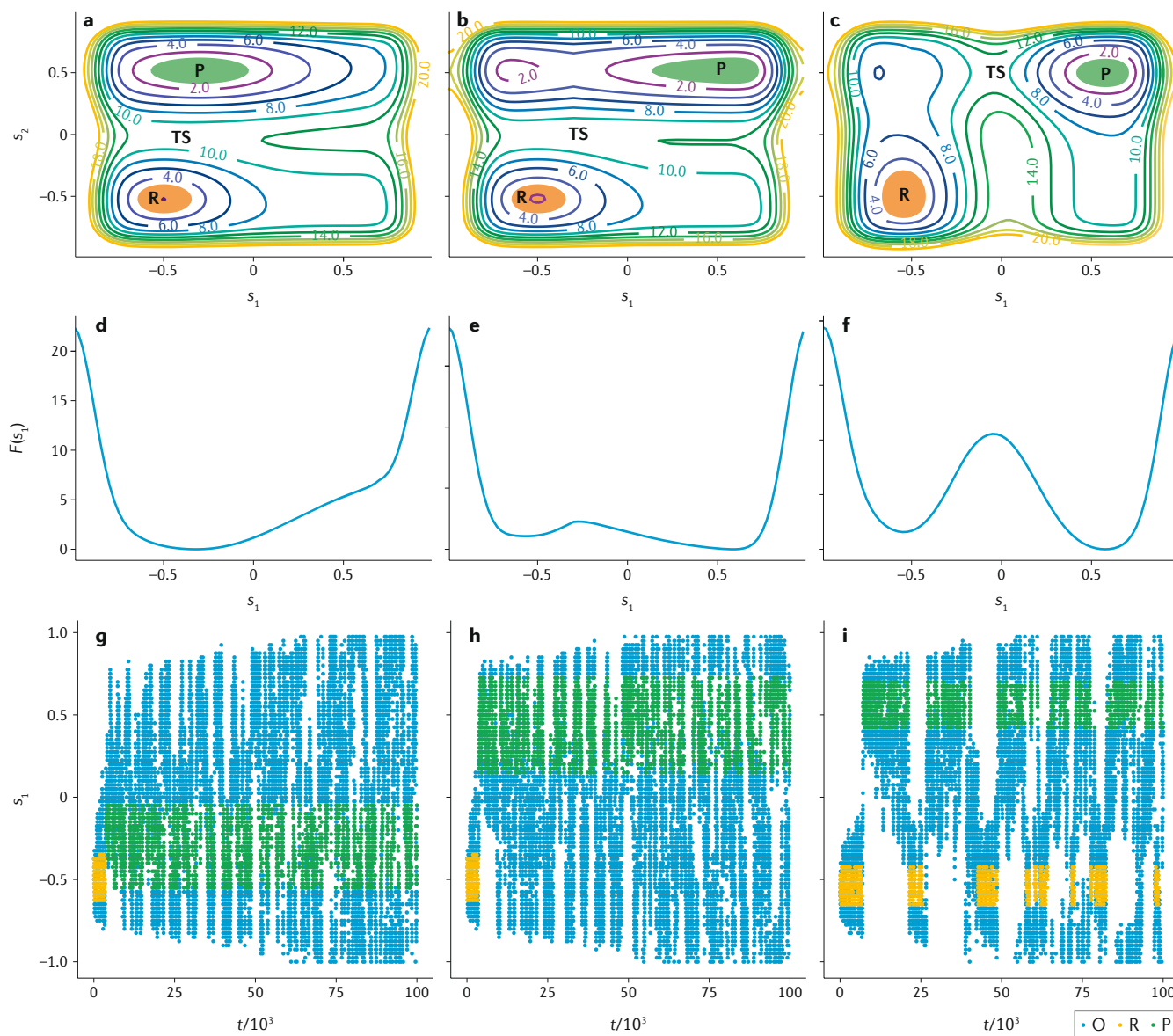


**Fig. 2 | Three potential energy landscapes, the corresponding free energies and metadynamics trajectories. a–c** | The three landscapes are representative of cases where the chosen collective variable (CV) cannot distinguish reactant (R) from product (P) (panel **a**), cannot distinguish the transition state (TS) from R (panel **b**) and can distinguish R, P and TS (panel **c**). The potential energy landscapes  $V(s_1, s_2)$  are shown as functions of two coordinates ( $s_1$  and  $s_2$ ) using contour lines. Regions within  $k_B T$  (where  $k_B$  is the Boltzmann constant) of the two metastable minima are coloured in orange (R state) and green (P state).  $s_1$  represents the chosen biased CV. **d–f** | The corresponding free energies  $F(s_1)$ . **g–i** | Metadynamics trajectories for  $s_1$ . Points are coloured by their location in the  $(s_1, s_2)$  space, with green and orange corresponding to the colours in panels **a–c**. Points that do not belong to the green and orange regions are shown in blue (O).  $t$ , time.

CVs are arbitrary functions of the atomic coordinates and, because they are usually fewer than the number of atomic coordinates, CVs provide a low-dimensional projection of the conformational space. For a multistable system, a minimum criterion for this low-dimensional projection is that different metastable states should correspond to different values of the CVs. If this condition is not satisfied (FIG. 2a), any bias potential added to one state will equally disfavour all the other states that correspond to the same value of the CVs (FIG. 2d). Even if the potential energy landscape has two minima, the free energy as a function of  $x$  has a single minimum. In this condition, metadynamics is not able to

accelerate in any manner the transitions between the two minima (FIG. 2g).

A second requirement is that the CVs should be able to distinguish transition states. Indeed, metadynamics tends to work in a similar manner to biological enzymes, in that it accelerates transitions by stabilizing the transition state relative to reactant and product states. If the CV distinguishes the metastable states, but not the transition state (FIG. 2b), the transition will not be enhanced. The corresponding free energy as a function of  $x$  (FIG. 2e) has two minima, but the value of the CV at the transition state approximately coincides with the value of the CV in states with lower free energy that are part of the basin of



attraction of reactants and products. In this case, under the action of metadynamics, the CV reaches a perfectly diffusive dynamics (FIG. 2h). However, this behaviour is not an indication of convergence: after the first transition is observed after approximately 5,000 steps, the dynamics explores only the product state and a secondary minimum. Therefore, the bias potential estimates the free energy without taking into account the reactant state. Indeed, the transitions between reactant and product are not enhanced at all by a bias acting on the CV, and transitions between reactant and product can happen due to only thermal fluctuations. As discussed below, in such a situation, the bias potential in equation 7 cannot be used to estimate the free energy. Instead, the well-tempered version of the bias, defined in equation 8, asymptotically provides a correct estimate. However, the bias does not accelerate the transition between the two minima, and therefore convergence is not substantially enhanced with respect to unbiased MD.

Metadynamics effectively works only if the CV takes different values in the metastable states and in the transition state between them (FIG. 2c). In other words, it must be possible to deduce with certainty from the value of the CV whether the system is in one metastable state or the other, or in the transition state. In this situation, metadynamics induces several transitions between the two metastable states (FIG. 2f,i), and the free energy can be reliably estimated from the bias in equation 7 or in equation 8.

A further requirement is that the number of employed CVs should not be too large. Filling a multidimensional space becomes more expensive as the dimensionality of the space grows. Because the overall idea of metadynamics is to disfavour the conformations that have been already visited, if the number of CVs is too large, the system will never return to exactly the same value of all the CVs. Approaches that employ replicas to allow a large number of CVs to be biased alternately<sup>21</sup> or simultaneously<sup>22</sup> can be used to alleviate this requirement. In the first case, bias-exchange metadynamics, each replica biases a single CV, so that a large number of CVs can be simultaneously probed. In the second case, multiple independent biases are constructed to flatten the distribution of multiple CVs using well-tempered metadynamics. All CVs are biased in all replicas, but the  $\Delta T$  parameter is modulated across the replica ladder, so that one replica provides unbiased sampling and the other replicas provide the capability to easily cross barriers. In both cases, coordinates are exchanged between replicas using an acceptance ratio that depends on the value of the biased CV of the different replicas. Another approach, parallel-bias metadynamics<sup>23</sup>, reproduces the character of bias-exchange metadynamics by using a single replica for which the weight (or probability) for each of the variables to be biased is computed on the fly, thus with the practical advantage of allowing simulation of a single replica.

Over the years, many other variants of metadynamics have been developed to address the problem of reconstructing the free energy in high dimensions.

- A popular strategy is to use a variable describing a path in a multidimensional CV space<sup>24,25</sup>, as discussed in the section on automatic determination of the CVs.

- In REF.<sup>26</sup>, metadynamics is combined with standard umbrella sampling to sample orthogonal CVs simultaneously.
- In REF.<sup>27</sup>, it is proposed to perform metadynamics on a 1D variable embedded in multidimensional CV space, the direction of which is learned on the fly during the simulation.
- In altruistic metadynamics<sup>28</sup>, the computational cost is reduced by simultaneously simulating multiple different molecular systems, predicting simultaneously their free-energy surfaces.
- In REF.<sup>29</sup>, the free-energy estimator of metadynamics and of adaptive force bias<sup>30</sup> are combined in a single history-dependent bias, substantially boosting convergence speed.
- Another variant of metadynamics has been developed to deal with the situation in which convergence is hindered by the presence of large free-energy basins stabilized by the entropy. This problem occurs in protein–ligand binding, for instance, for which an entropic bottleneck arises from the need of the ligand to find its way to the binding pocket. In such cases, in which these bottlenecks are known a priori, their effect can be moderated by setting proper restraints<sup>31</sup>.

Finally, we note that although metadynamics was initially introduced to explore and reconstruct the free energy along biased variables, by suitable re-weighting techniques<sup>32–35</sup> it can also be used to reconstruct the free energy along non-biased variables. However, in these cases, one should pay particular attention to make sure that analysed variables are sufficiently sampled.

## Computing the free energy and its error

The manner of estimating the free energy and controlling the error is different in ordinary metadynamics and in its well-tempered variant. Therefore, we consider these two cases separately.

**Ordinary metadynamics.** In ordinary metadynamics, if the CVs are well chosen, after a time  $t_{\text{fill}}$  all the free-energy minima are filled with Gaussians and the dynamics becomes diffusive in CV space (FIG. 2i). After this time, the bias potential continues to change, because new Gaussians are added again and again. However,  $B_t(s)$  becomes stationary, that is, its shape remains qualitatively the same at different times (Supplementary Fig. 1).  $B_t(s)$  behaves like an ordinary observable in a finite-temperature molecular simulation: after a transient time (the equilibration time), the observable does not remain constant, but keeps on fluctuating. A meaningful estimator of its thermodynamic average is the time average. Similarly, in metadynamics, the instantaneous value of the bias potential is not meaningful, but rather its time average after  $t_{\text{fill}}$ , which plays the role of an equilibration time. Therefore, at time  $t$  the best estimator of the negative of the free energy is

$$\bar{B}_t(s) = \frac{1}{t - t_{\text{fill}}} \sum_{t'=t_{\text{fill}}}^t B_{t'}(s) \quad (9)$$

This average converges exactly to  $-F(s)$  for  $t \rightarrow \infty$  if the dynamics in the CV is adiabatically separated from the dynamics in the other variables<sup>17,36</sup>. Even if this condition is violated, if transitions between reactants and products are observed on a timescale compatible with diffusion on a flat landscape, the average in equation 9 converges to the free energy within numerical accuracy. This has been verified numerically in a metadynamics simulation of a lattice model in which the free energy is known analytically<sup>37</sup>. However, if under the action of metadynamics transitions between reactants and products happen only rarely (FIG. 2h), the time average is not guaranteed to converge to the negative of the free energy. In particular, transitions should be considered as rare if they happen on a timescale that is comparable to that of an unbiased plain MD simulation, which implies that they are not accelerated by the metadynamics bias. We remark that if in a metadynamics simulation one observes a behaviour like that in FIG. 2h, one should conclude that the CV is not appropriate, stop the simulation and look for a more appropriate variable.

The statistical accuracy of the estimator in equation 9 is controlled by the same techniques used to monitor the accuracy of the average value of an observable in a finite-temperature run. For example, one can perform a block analysis by first splitting the simulation time after  $t_{\text{fill}}$  in blocks and estimating the error by looking at the difference in the average bias potentials in the blocks. One can then monitor how the error estimator depends on the number of blocks. If the total averaging time  $t - t_{\text{fill}}$  is substantially larger than the correlation time, the error estimate will be approximately independent of the number of blocks (Supplementary Fig. 1).

**Well-tempered metadynamics.** A similar analysis can be performed for well-tempered metadynamics. However, in this case, the changes in the bias potential itself are not a good indication of the convergence of the simulation, because, by construction, the increments in the bias potential become smaller and smaller as the simulation progresses. Qualitatively, it is necessary to check that, even if the bias potential becomes quasi-constant, the system still undergoes transitions between the relevant free-energy minima. Quantitatively, these transitions can be observed by performing a block analysis of the histogram of the biased CV. Indeed, the standard free-energy estimator used in well-tempered metadynamics can be replaced with the standard umbrella sampling formula  $F(s) = -T \log H(s) - V(s)$ , where  $H$  is the histogram of the visited points in the CV space, which must be computed with a proper smoothing<sup>33</sup>. This procedure is equivalent to re-weighting each visited frame of coordinates  $q$  with a factor proportional to  $\exp(V(s(q), t_{\text{final}})/T)$ , where  $t_{\text{final}}$  is the simulation length. The error on the free energy can be estimated by:

- Discarding a suitable initial part of the simulation, during which the main free-energy wells are filled
- Breaking the following part of the simulation into blocks and computing the histogram of the CVs in each block, and its error, using block analysis
- Converting the error on the histogram to an error on the free-energy estimator.

In particular, the error on the histogram can be computed by exploiting the relationship between the bias potential and the histogram itself<sup>8</sup>, that is,  $N(s) \propto C + \exp(\frac{V(s)}{\Delta T})$ , where  $C$  is an arbitrary constant. The histogram accumulated in the  $i$ th block is thus proportional to  $\exp(\frac{B(s, t_{\text{fill}} + (i+1)L_b)}{\Delta T}) - \exp(\frac{B(s, t_{\text{fill}} + iL_b)}{\Delta T})$ , where  $L_b$  is the length of the block. The error on the free energy can thus be estimated as

$$\frac{1}{\sqrt{N_b}} \sqrt{\text{Var}_i \left[ \log \left( e^{\frac{B(s, t_{\text{fill}} + (i+1)L_b)}{\Delta T}} - e^{\frac{B(s, t_{\text{fill}} + iL_b)}{\Delta T}} \right) \right]} \quad (10)$$

where  $N_b$  is the number of blocks and the variance should be computed across all the blocks (Supplementary Fig. 1).

The free-energy differences between reactants and products evaluated for two of the model systems shown in FIG. 2 are reported in Supplementary Table 1. In particular, in the simpler case in which CVs correctly identify the transition state as well as the reactant and product states, both methods provide a correct estimate. However, in the more difficult case in which CVs cannot identify the transition state, ordinary metadynamics provides a biased result and well-tempered metadynamics requires a simulation time comparable to the one of standard MD to converge to the correct result.

### Automatic learning of CVs

As discussed, cases in which metadynamics does not converge or converges to an incorrect result can be often ascribed to a common problem: the chosen CVs do not correctly describe the relevant barriers, a problem that is easy to detect if the simulation is analysed properly. On encountering this problem, metadynamics practitioners need to search for a ‘better’ CV capable of describing correctly the conformational change of interest. This need perhaps explains why many different CVs have been developed in recent years, especially in the community using metadynamics. Here, we review recently developed approaches for ‘learning’ the correct CVs automatically. These are summarized in TABLE 1.

We first describe the so-called path CVs<sup>24,25</sup>. These variables are based on the definition of a series of reference structures for the system under investigation. If a transition from a state A to a state B is to be studied, these reference structures are ideally located between A and B (FIG. 3). A progressive CV is then defined using the following exponential average

$$s(r) = \frac{\sum_i i e^{-\lambda d_i}}{\sum_i e^{-\lambda d_i}} \quad (11)$$

where  $d_i$  is the squared distance between the current atomic configuration and the  $i$ th reference structure, and  $\lambda$  is a smoothing parameter. This exponential average identifies which of the reference structures is closest to the current one and assigns to the CV a value that interpolates between the indexes of those structures. A metadynamics simulation can then be used to enforce transitions between A and B and vice versa by biasing this CV. The procedure can be generalized to vector indexes

rather than scalar ones to allow for a higher-dimensional embedding of the configurational space<sup>38</sup>. Importantly, it is possible to optimize the location of the landmark structures through an iterative series of simulations. This can be done using a procedure<sup>24</sup> inspired by the nudged-elastic-band method<sup>39</sup>. At each new simulation, the reference structures are changed to become more similar to the real intermediates observed in the MD simulation. The actual definition of the CV is thus different at every new iteration. Ideally, the intermediate structures relax towards a path that passes through the transition state and, after a sufficient number of iterations, a metadynamics simulation biasing this CV is able to make the system diffuse from A to B and vice versa. In REF.<sup>25</sup>, a progression CV with a definition similar to equation 11 was introduced. In this case, however, the definition of the path CV is evolved during the metadynamics simulation, potentially speeding up the search for the optimal path.

The function defined in equation 11 allows a high-dimensional representation (coordinates of the atoms) to be reduced to a lower-dimensional one (a single CV). More generally, arbitrary features can be used as a starting point for a dimensional reduction of this type. Clearly, if some prior knowledge is available, it is possible to exploit it to define the distances  $d_i$  in an already reduced space. All the automatic methods used to construct CVs are based on the idea of constructing a small number of linear or nonlinear functions of a larger set of features that are chosen a priori.

One of the possible criteria used in dimensional reduction algorithms is that of preserving the distance between structures computed using the full set of coordinates. This is what is done in classic multidimensional scaling, for instance<sup>40</sup>. However, distances between structures are typically informative only for a narrow range of values. Diffusion maps can be used to tackle this issue<sup>41</sup>. In this method, a fictitious random walk connecting microstates that are close to each other in the initial feature space is constructed, and the slow modes of this random walk are assigned as the larger distances in the low-dimensional representation. The sketch-map algorithm instead constructs a low-dimensional embedding in which only distances in a selected range are preserved

in the procedure. Specifically, sigmoid functions of the distances in the initial feature space are used to tune the distance range that is considered relevant for the dimensional reduction<sup>42</sup>.

Recently, procedures inspired by machine learning have been used to design variables that are capable of distinguishing reactants and products. Indeed, CVs of this type are closely related to representations provided by supervised learning algorithms, in which a parametric representation is optimized to correctly distinguish labelled examples that are provided in advance. For instance, support vector machines and logistic regressions have been used to classify folded and unfolded states of a protein, with the classifier then used as a CV to perform enhanced sampling<sup>43</sup>. A similar approach based on linear-discriminant analysis has also been used<sup>44</sup>. This latter approach was applied to the characterization of chemical reactions, for example<sup>45,46</sup>.

The methods discussed above aim at either finding a low-dimensional embedding that correctly represents the structures seen in a preliminary run, or distinguishing pre-assigned basins in the energetic landscape of the system. However, these methods do not explicitly take into account how good these variables would be for representing the kinetics of the system. The ideal CV for describing a transition between two metastable states R and P is the so-called committor function<sup>47</sup>. The committor of a configuration  $x$  to the metastable state R is the probability that a trajectory starting from  $x$  reaches the state R before P. Finding the committor explicitly is possible in only simple model systems, but several approaches have been developed to estimate its value, and parameterize the committor<sup>48</sup>. These approaches can in principle be used to find an appropriate CV to perform metadynamics.

As discussed above, good CVs typically exhibit large free-energy barriers that are removed when an incorrect dimensional reduction is done, because such dimensional reduction mixes the true transition states with other more stable states. The idea of spectral gap optimization<sup>49</sup> is to select linear combinations of putative CVs and choose the one with the slowest transition rate between two minima. Under the assumption that different CVs have comparable diffusion constants, this would

Table 1 | Comparison of methods for automatically finding CVs

Method	Advantages	Disadvantages	
Path CV <sup>24,25,38</sup>	Allows the description of complex reaction pathways; can be iteratively optimized	Requires knowledge of the initial and final states	
Committor parameterization <sup>48</sup>	Provides the best possible reaction coordinate	Requires knowledge of the initial and final states; requires running many short MD trajectories and can be very costly	
Spectral gap optimization <sup>49</sup>	Simple and computationally cheap	Requires knowledge of the initial and final states; finds the best variable in a set, but does not allow parameterization of a new one	
Machine learning	Distribution based <sup>41–46</sup>	Only requires ensemble averages	Resulting CVs might suboptimally describe barriers
	Dynamics based <sup>50,51,53–55</sup>	Explicitly takes into account the kinetics of the system	Requires long unbiased trajectories or re-weighting methods

CV, collective variable; MD, molecular dynamics.



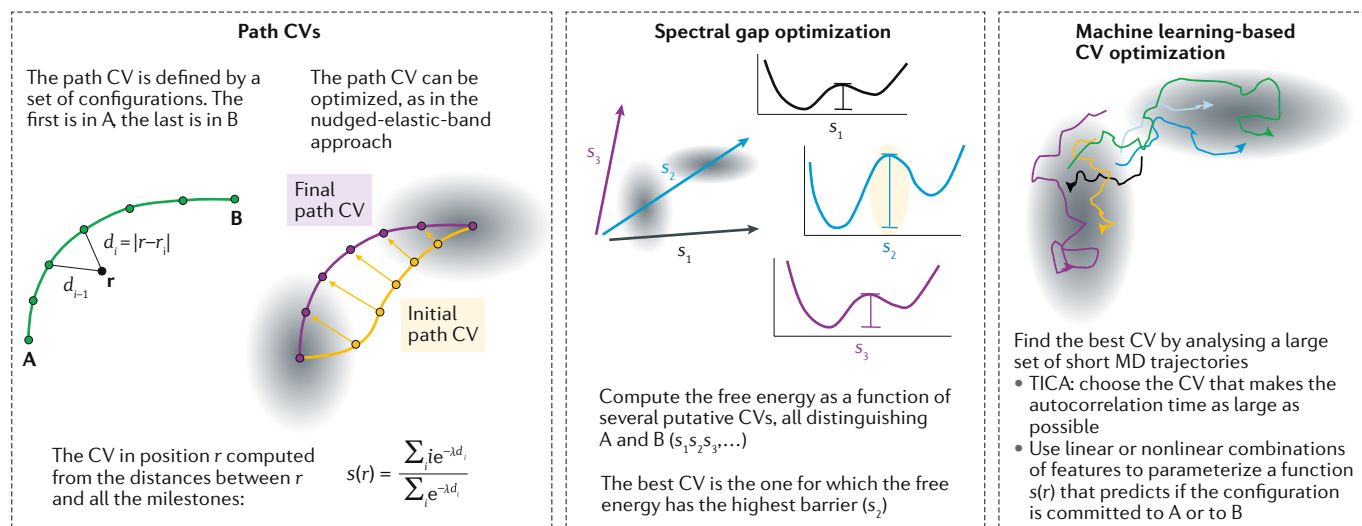


Fig. 3 | **Three approaches for automatically finding the best CV.**  $d_i$  is the squared distance between the current atomic configuration and the  $i$ th reference structure, and  $\lambda$  is a smoothing parameter.  $r$  represents the present coordinates of the system, and  $r_i$  the coordinates in the  $i$ th milestone.  $s_1, s_2$  and  $s_3$  represent possible collective variables (CVs). MD, molecular dynamics; TICA, time-independent component analysis.

be the one with the largest barrier separating reactants and products (FIG. 3b). To recover the free energy along putative linear combinations, it is crucial to perform a proper re-weighting. With a similar goal to spectral gap optimization, time-independent component analysis (TICA) constructs a linear combination of pre-selected features that is ‘as slow as possible’, that is, with the largest possible autocorrelation time. The first few components of a pre-computed TICA can be used as biased CVs for metadynamics<sup>50</sup>. A TICA-based approach was also introduced in REF<sup>51</sup>, in which the time-independent components (TICs) are directly computed during the biased simulation, thus allowing conformational changes that are only visible in biased sampling to be studied. We note that metadynamics performed with the correct CV changes the relaxation dynamics of the system substantially because, ideally, the slowest dynamics takes place in the hyperplane of a constant CV. Therefore, to compute the correct TICs, it is necessary to apply a re-weighting technique. The method of REF<sup>51</sup> was used to identify slow molecular motions in complex chemical reactions<sup>52</sup>. Following a similar idea, it was recently shown that variational auto-encoders can be used to construct nonlinear functions that optimally represent the kinetics of the system<sup>53,54</sup>. A related approach was used in REF<sup>55</sup>, in which a linear encoder was combined with a nonlinear decoder. In principle, limiting the encoder step to linear combinations allows the generated CVs to be easier to interpret.

### Implementation

CVs are often defined by complicated functional forms, but they usually depend on the coordinates of a limited number of atoms. Moreover, the same CVs and the same variants of metadynamics can be used across different applications, such as *ab initio* and classical MD. For this reason, metadynamics is optimally implemented in a separate library — such as PLUMED<sup>56</sup>, COLVAR<sup>57</sup> or

SSAGES<sup>58</sup> — which can then be used in combination with any MD code (TABLE 2). These libraries typically have their own input files that are read during initialization and are then called at every iteration of the MD simulation (FIG. 4). Coordinates should be passed to the library. In some cases, this might lead to a slow down of the simulation, in particular if the MD engine stores the coordinates on a graphical processing unit but the library requires coordinates on the central processing unit. The library then computes the requested CVs and bias potentials, resulting in forces that should be added to those computed by the MD engine. In principle, metadynamics can also be used with MC simulations, although we are not aware of MC codes interfaced with the above-mentioned libraries.

The typical aim of these libraries is to allow a user to add arbitrary bias potentials on chosen CVs. In particular, substantial flexibility is usually given to the user in the choice of the CVs, because tuning their definition — either manually or automatically, as discussed above — is a crucial step in the application of any biasing technique. The code should then compute the derivatives of the  $i$ th CV  $s_i$  with respect to the atomic positions.

Arbitrary combinations of CVs can also be used. At least two of the above-mentioned packages, COLVAR and PLUMED<sup>56,57</sup>, allow users to specify arbitrary algebraic functions in their input that are then automatically differentiated. The possibility of using arbitrary combinations of CVs makes it possible to implement some of the automatically determined CVs discussed above directly in the input script. Although this option is often suboptimal from the performance point of view, it speeds up the development of new ideas.

The same approach can be used to implement any method based on the idea of adding a bias potential or a force to a set of chosen CVs. This is the reason why these packages typically provide the user with many other enhanced sampling methods based on biasing CVs, such

Table 2 | Availability of metadynamics in commonly used MD codes

MD code	Native	PLUMED	COLVARS	SSAGES
ACEMD <sup>68</sup>	No	Yes	No	No
AMBER <sup>69</sup>	No	Yes	No	No
CP2K <sup>70</sup>	Yes	Yes	No	No
DLPOLY <sup>71</sup>	No	Yes	No	No
DESMOND <sup>72</sup>	Yes	No	No	No
GROMACS <sup>73</sup>	No	Yes	Yes	Yes
i-Pi <sup>74</sup>	No	Yes	No	No
HOOMD <sup>75</sup>	No	No	No	Yes
LAMMPS <sup>76</sup>	Yes <sup>a</sup>	Yes	Yes	Yes
NAMD <sup>77</sup>	Yes <sup>b</sup>	Yes	Yes	No
OPENMD <sup>78</sup>	No	No	No	Yes
OPENMM <sup>79</sup>	Yes	Yes	No	No
ORAC <sup>80</sup>	Yes	No	No	No
PINY-MD <sup>81</sup>	No	Yes	No	No
QUANTUM-ESPRESSO <sup>82</sup>	No	Yes	No	No
QBOX <sup>83</sup>	No	No	No	Yes

The 'native' column refers to implementations of metadynamics that do not require any additional libraries. Compatibility with the three libraries discussed in this Technical Review is also indicated. Notice that these three libraries are currently under development and that this table reflects the respective documentation in October 2019. MD, molecular dynamics. <sup>a</sup>A copy of the COLVARS code is included in the official LAMMPS repository. <sup>b</sup>A copy of the COLVARS code is included in the official NAMD repository.

as umbrella sampling<sup>1</sup>, steered MD<sup>59</sup> or other techniques that have been developed more recently.

Furthermore, whereas the calculation of metadynamics forces can be implemented by explicitly summing the history of visited conformation (as in equation 7), the computational cost is usually substantially decreased by accumulating the sum of Gaussian functions on a grid, so that cost of the calculation of the forces is independent of the simulation length. The bias potential stored on the grid is updated using equation 6 and its cost grows exponentially with the number of biased CVs. For this reason, it is convenient to use interpolation schemes that make it possible to use grids that are less dense, thus accelerating the update of the potential.

The availability of the discussed features in the libraries PLUMED, COLVAR and SSAGES is summarized in TABLE 3. The PLUMED package is the most complete in terms of support for metadynamics variants, because it was developed by a community centred around the developers of the method, can be loaded at runtime as a plugin, and implements a number of analysis and post-processing tools that might be crucial for dealing with advanced methods. The COLVARS package can be extended using tool command language and some of the unsupported features might be implemented using scripts that have been made available by the community. Finally, the SSAGES package is still at a pre-release stage and thus its support is relatively limited. The documentation of these three packages can also be considered as a starting point to explore the wide range of CVs used in the literature. The PLUMED community has recently made available a public repository named PLUMED-NEST containing data needed to reproduce enhanced sampling simulations, which can also be of great use to new users<sup>60</sup>.

## Discussion and perspectives

Because of the success of metadynamics, several variants have been developed over the years, as discussed above. A question that naturally arises in applications is which variant should be used.

A preliminary observation is that the convergence of well-tempered metadynamics has been proved rigorously in any condition and for any possible choice of the CV. Indeed, in this method, the bias potential asymptotically does not change, making the approach technically equivalent to ordinary umbrella sampling. The approach requires choosing an extra parameter, the effective temperature  $\Delta T$  in equation 8, whose optimal value depends on the height of the relevant barriers, which may not be known. A possible way to overcome the problem of choosing this parameter has been proposed<sup>61</sup>. However, as we already underlined, if the CV is not correctly chosen, the convergence speed of well-tempered metadynamics is similar to that of ordinary MD, making it not useful.

Ordinary metadynamics is instead a process in which the dynamics happens in an extended space, including not only the coordinates but also the bias potential. This dynamics has the advantage of enforcing diffusion in the CV even when the latter is not correct. The properties of this dynamics have not yet been fully understood, and its convergence was rigorously proved only in conditions of adiabatic separation of the CV dynamics<sup>17</sup>. If this condition is violated, systematic errors may arise, such as those observed in the examples described in this Technical Review, and as rigorously proven in REF.<sup>62</sup>. However, if the CVs are appropriately chosen, these errors are in practice well below the statistical accuracy of the free-energy estimator<sup>37</sup>. Furthermore, in practical applications, in which adiabatic separation is often violated, it can be convenient to reconstruct the free energy a posteriori, not as an average of the bias potential, but using estimators based

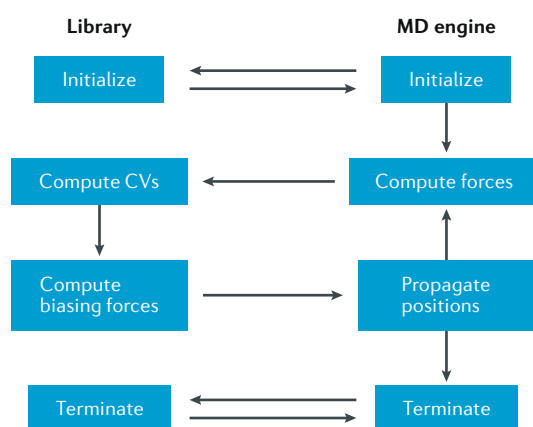


Fig. 4 | Typical architecture of a library to perform metadynamics simulations. The library is initialized at the beginning of the simulation and usually needs a separate input file that specifies the options needed to perform metadynamics. At each step, coordinates are passed from the molecular dynamics (MD) engine to the library and additional forces are returned and added to the physical forces computed by the MD engine. The library is then finalized at the end of the simulation. CV, collective variable.

Table 3 | Feature comparison of MTD libraries

MTD feature	PLUMED	COLVARS	SSAGES
Ordinary MTD	Yes	Yes	Yes
WT-MTD	Yes	Yes	No
Grids	Yes	Yes	Yes
Multiple walkers	Yes	Yes	Yes
Bias exchange	Yes <sup>a</sup>	No	No
Arbitrary CVs	Yes	Yes	No

These three libraries are currently under development. This table reflects the respective documentation in October 2019. CV, collective variable; MTD, metadynamics; WT, well-tempered. <sup>a</sup>Only in combination with GROMACS.

on the mean force observed during the biased run<sup>57,63</sup> or Gaussian process regression<sup>64</sup>.

To understand better the differences between these approaches, it is important to discuss what happens if the CVs are not appropriately chosen. In FIG. 2, we presented three examples of 2D potential energy landscapes associated with systems with two metastable states. In two cases, in particular, the free energy as a function of the  $s_1$  coordinate is very similar: two minima separated by a barrier (FIG. 2b,c). However, the capability of the method of estimating the free energy is strikingly different in the two cases. In one case, estimating the free energy is practically impossible: the CV identifies the two metastable states, but not the transition state between the two, and therefore the bias potential does not accelerate the transitions (FIG. 2e,h). In FIG. 5a, we show a potential energy landscape characterized by the presence of four minima. The free-energy landscapes as a function of  $x$  and  $y$  (FIG. 5b) are approximately flat, despite the presence of very substantial barriers in the 2D landscape. In this case, if  $x$  is used as a CV, well-tempered

metadynamics is by construction unable to generate a bias potential that can enhance the sampling in the  $x$  direction; similarly if  $y$  is used as a CV. Indeed, at convergence, the bias potential is a constant, and this bias is not affected any longer by the new Gaussians, whose height becomes smaller and smaller at the end of the run. Therefore, the system will get stuck in one of the minima. In short, the problem is that a bias potential compensating exactly the free energy does not necessarily make the landscape barrierless. The behaviour of ordinary metadynamics on this system is rather different: the approach by construction enforces transitions even when the CV is not correct, as long as the CV takes different values in the different minima. The system continues to perform transitions and explore the free-energy landscape. However, the bias potential is affected by large fluctuations, and the free-energy estimate does not converge. Indeed, because the transition states are not identified correctly by the CV, forward and backward transitions might follow different paths, leading to hysteresis in the estimated free energy.

A possible way out of this problem is offered by replica exchange methods. Metadynamics can be combined with parallel tempering<sup>65</sup>, CV tempering<sup>22</sup> or solute tempering<sup>66</sup> to enhance sampling in directions that are not directly biased. These approaches address, to some extent, the problem of metastability in degrees of freedom that are orthogonal to the biased CV. Another way to address the same problem is to use bias-exchange metadynamics<sup>21</sup>, an approach in which several metadynamics simulations are run in parallel and at the same temperature, each biasing a different CV. Exchanges of the coordinates between different replicas are attempted at regular time intervals, and accepted according to the Metropolis criterion. This approach makes it possible to use a very large number of CVs simultaneously, and

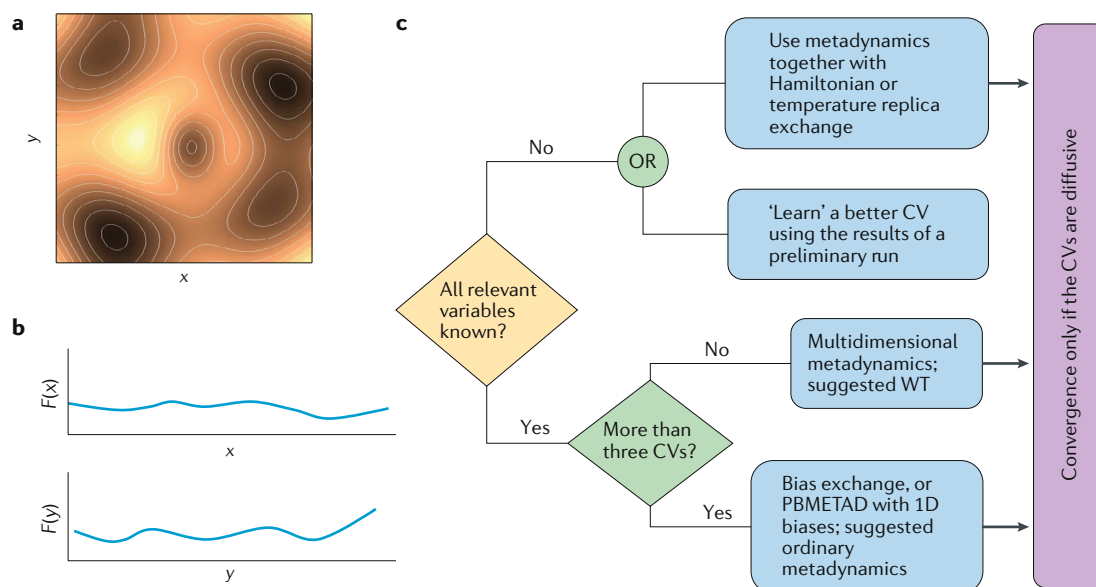


Fig. 5 | **Choosing the correct metadynamics variant.** **a, b** | An example of a potential energy landscape characterized by the presence of deep minima (panel **a**), but whose free energy  $F$  as a function of two variables ( $x$  and  $y$ ) is approximately flat (panel **b**). This situation is rather common in practical applications. **c** | A decision tree for choosing the most appropriate version of metadynamics. CV, collective variable; PBMETAD, parallel-bias metadynamics; WT, well-tempered.

dramatically reduces the hysteresis if all the relevant CVs are biased in at least one replica.

Using replica bias exchange in combination with well-tempered metadynamics is delicate, because in this approach the simplest way to check whether the simulation is meaningful requires verifying that at the end of the simulation the system is able to diffuse through all the regions in which one wants to estimate the free energy. In a situation like the one depicted in FIG. 5a, if a single replica is used, the CV tends to freeze in one of the local minima. If any replica exchange method is used, an accepted exchange move can induce a jump of the CV from one minimum to another. However, these jumps are not sufficient to ensure that the free-energy estimator is correct. Instead, it should be verified that continuous trajectories, travelling across the space of available replicas, display transitions between the relevant states.

These considerations form a basis for some guidelines for choosing among the different versions of metadynamics (FIG. 5c). In our opinion, the well-tempered version of metadynamics offers some advantages for estimating the free energy as a simultaneous function of two or more CVs. Indeed, this approach has been proved to converge rigorously, and makes it possible to perform the calculation without defining explicitly the region in which the free energy should be estimated: one simply chooses the maximum value of the free energy that one considers interesting, and the approach automatically fills the free-energy minima to approximately that level. If one uses ordinary metadynamics to estimate the free energy in a multidimensional domain, one should fix the appropriate boundary conditions, restricting the dynamics in the domain<sup>6,37,67</sup>. If the correct CV is unknown, it may be appropriate to use a method combining metadynamics and replica exchange. In bias-exchange metadynamics, an arbitrarily large number of CVs can be biased simultaneously. Because ordinary metadynamics forces transitions

even when the CV is not correct, by using it in a bias-exchange scheme it is possible to converge to a low-dimensional free-energy estimate even in the condition of FIG. 5, where the free energy projected on a single variable is almost barrierless despite the presence of metastable states. Well-tempered metadynamics instead might remain stuck unless the CV describes very well the transition state. Therefore, we see some advantages in using ordinary metadynamics with respect to the well-tempered version in bias-exchange methods.

The usefulness of metadynamics (and of any enhanced sampling method based on biasing CVs) is largely determined by its capability to identify an appropriate CV that describes the relevant transitions. Historically, CVs have been searched for by trial and error, and their discovery has been part of the process of understanding the system under investigation. In our opinion, going beyond this protocol is the frontier of enhanced sampling methods. The community is well aware of the importance of this problem: recently, a number of approaches for the automatic search of CVs have been proposed, including approaches inspired by machine learning, as we discuss above. Automatic training procedures allow the use of functions of arbitrary complexity, such as artificial neural networks. Although this can bring important progress, one should also consider that complex functional forms might be difficult to interpret and, in the end, could teach less about the investigated system. In addition, highly flexible functional forms might easily lead to situations where data are overfitted. We thus believe that finding a solution to the problem of automatically finding CVs while ensuring the appropriate balance between accuracy, generality and interpretability, is still an open problem that will likely attract a lot of interest in the near future.

Published online: 06 March 2020

- Torrie, G. M. & Valleau, J. P. Nonphysical sampling distributions in Monte Carlo free-energy estimation: umbrella sampling. *J. Comput. Phys.* **23**, 187–199 (1977).
- Laio, A. & Parrinello, M. Escaping free energy minima. *Proc. Natl Acad. Sci. USA* **99**, 12562–12566 (2002).
- Laio, A. & Gervasio, F. L. Metadynamics: a method to simulate rare events and reconstruct the free energy in biophysics, chemistry and material science. *Rep. Prog. Phys.* **71**, 126601 (2008).
- Barducci, A., Bonomi, M. & Parrinello, M. Metadynamics. *Wiley Interdiscip. Rev. Comput. Mol. Sci.* **1**, 826–843 (2011).
- Sutto, L., Marsili, S. & Gervasio, F. L. New advances in metadynamics. *Wiley Interdiscip. Rev. Comput. Mol. Sci.* **2**, 771–779 (2012).
- Baftizadeh, F., Cossio, P., Pietrucci, F. & A. L. Protein folding and ligand–enzyme binding from bias-exchange metadynamics simulations. *Curr. Phys. Chem.* **2**, 79–91 (2012).
- Bussi, G. & Branduardi, D. Free-energy calculations with metadynamics: theory and practice. *Rev. Comput. Chem.* **28**, 1–49 (2015).
- Valsson, O., Tiwary, P. & Parrinello, M. Enhancing important fluctuations: rare events and metadynamics from a conceptual viewpoint. *Annu. Rev. Phys. Chem.* **67**, 159–184 (2016).
- Theodoropoulos, C., Qian, Y.-H. & Kevrekidis, I. G. Coarse stability and bifurcation analysis using time-steppers: a reaction-diffusion example. *Proc. Natl Acad. Sci. USA* **97**, 9840–9843 (2000).
- Grubmüller, H. Predicting slow structural transitions in macromolecular systems: conformational flooding. *Phys. Rev. E* **52**, 2893–2906 (1995).
- Glover, F. Future paths for integer programming and links to artificial intelligence. *Comput. Oper. Res.* **13**, 533–549 (1986).
- Cvijović, D. & Klinowski, J. Taboo search — an approach to the multiple minima problem. *Science* **267**, 664–666 (1995).
- Huber, T., Torda, A. E. & Van Gunsteren, W. F. Local elevation: a method for improving the searching properties of molecular dynamics simulation. *J. Comput. Aided Mol. Des.* **8**, 695–708 (1994).
- Wang, F. & Landau, D. Efficient, multiple-range random walk algorithm to calculate the density of states. *Phys. Rev. Lett.* **86**, 2050 (2001).
- Mezei, M. Adaptive umbrella sampling: self-consistent determination of the non-Boltzmann bias. *J. Comput. Phys.* **68**, 237–248 (1987).
- Rosenblatt, M. Remarks on some nonparametric estimates of a density function. *Ann. Math. Stat.* **27**, 832–837 (1956).
- Bussi, G., Laio, A. & Parrinello, M. Equilibrium free energies from nonequilibrium metadynamics. *Phys. Rev. Lett.* **96**, 090601 (2006).
- Barducci, A., Bussi, G. & Parrinello, M. Well-tempered metadynamics: a smoothly converging and tunable free-energy method. *Phys. Rev. Lett.* **100**, 020603 (2008).
- Spall, J. C. *Introduction to Stochastic Search and Optimization* (Wiley, 2003).
- Dama, J. F., Parrinello, M. & Voth, G. A. Well-tempered metadynamics converges asymptotically. *Phys. Rev. Lett.* **112**, 240602 (2014).
- Piana, S. & Laio, A. A bias-exchange approach to protein folding. *J. Phys. Chem. B* **111**, 4553–4559 (2007).
- Gil-Ley, A. & Bussi, G. Enhanced conformational sampling using replica exchange with collective-variable tempering. *J. Chem. Theory Comput.* **11**, 1077–1085 (2014).
- Pfaendtner, J. & Bonomi, M. Efficient sampling of high-dimensional free-energy landscapes with parallel bias metadynamics. *J. Chem. Theory Comput.* **11**, 5062–5067 (2015).
- Branduardi, D., Gervasio, F. L. & Parrinello, M. From A to B in free energy space. *J. Chem. Phys.* **126**, 054103 (2007).
- Leines, G. D. & Ensing, B. Path finding on high-dimensional free energy landscapes. *Phys. Rev. Lett.* **109**, 020601 (2012).
- Awasthi, S., Kapil, V. & Nair, N. Sampling free energy surfaces as slices by combining umbrella sampling and metadynamics. *J. Comp. Chem.* **37**, 1413–1424 (2016).
- Marinelli, F. Following easy slope paths on a free energy landscape: the case study of the Trp-cage folding mechanism. *Biophys. J.* **105**, 1236–1247 (2013).
- Hošek, P., Toulcová, D., Bortolato, A. & Spiwok, V. Altruistic metadynamics: multisystem biased simulation. *J. Phys. Chem. B* **120**, 2209–2215 (2016).
- Fu, H. et al. Zooming across the free-energy landscape: shaving barriers, and flooding valleys. *J. Phys. Chem. Lett.* **9**, 4738–4745 (2018).
- Darve, E. & Pohorille, A. Calculating free energies using average force. *J. Chem. Phys.* **115**, 9169–9183 (2001).
- Limongelli, V., Bonomi, M. & Parrinello, M. Funnel metadynamics as accurate binding free-energy method. *Proc. Natl Acad. Sci. USA* **110**, 6358–6363 (2013).



32. Bonomi, M., Barducci, A. & Parrinello, M. Reconstructing the equilibrium Boltzmann distribution from well-tempered metadynamics. *J. Comput. Chem.* **30**, 1615–1621 (2009).
33. Branduardi, D., Bussi, G. & Parrinello, M. Metadynamics with adaptive Gaussians. *J. Chem. Theory Comput.* **8**, 2247–2254 (2012).
34. Tiwary, P. & Parrinello, M. A time-independent free energy estimator for metadynamics. *J. Phys. Chem. B* **119**, 736–742 (2014).
35. Donati, L. & Keller, B. G. Girsanov reweighting for metadynamics simulations. *J. Chem. Phys.* **149**, 072335 (2018).
36. Iannuzzi, M., Laio, A. & Parrinello, M. Efficient exploration of reactive potential energy surfaces using Car-Parrinello molecular dynamics. *Phys. Rev. Lett.* **90**, 238302 (2003).
37. Crespo, Y., Marinelli, F., Pietrucci, F. & Laio, A. Metadynamics convergence law in a multidimensional system. *Phys. Rev. E* **81**, 055701 (2010).
38. Spiwok, V. & Králová, B. Metadynamics in the conformational space nonlinearly dimensionally reduced by Isomap. *J. Chem. Phys.* **135**, 224504 (2011).
39. Henkelman, G., Uberuaga, B. P. & Jónsson, H. A climbing image nudged elastic band method for finding saddle points and minimum energy paths. *J. Chem. Phys.* **113**, 9901–9904 (2000).
40. Cox, T. F. & Cox, M. A. *Multidimensional Scaling* (Chapman and Hall/CRC, 2000).
41. Rohrdanz, M. A., Zheng, W., Maggioni, M. & Clementi, C. Determination of reaction coordinates via locally scaled diffusion map. *J. Chem. Phys.* **134**, 124116 (2011).
42. Tribello, G. A., Ceriotti, M. & Parrinello, M. Using sketch-map coordinates to analyze and bias molecular dynamics simulations. *Proc. Natl Acad. Sci. USA* **109**, 5196–5201 (2012).
43. Sultan, M. M. & Pande, V. S. Automated design of collective variables using supervised machine learning. *J. Chem. Phys.* **149**, 094106 (2018).
44. Mendels, D., Piccini, G., Brotzakis, Z. F., Yang, Y. I. & Parrinello, M. Folding a small protein using harmonic linear discriminant analysis. *J. Chem. Phys.* **149**, 194113 (2018).
45. Piccini, G. & Parrinello, M. Accurate quantum chemical free energies at affordable cost. *J. Phys. Chem. Lett.* **10**, 3727–3731 (2019).
46. Rizzi, V., Mendels, D., Sicilia, E. & Parrinello, M. Blind search for complex chemical pathways using harmonic linear discriminant analysis. *J. Chem. Theory Comput.* **15**, 4507–4515 (2019).
47. Vanden-Eijnden, E. Transition-path theory and path-finding algorithms for the study of rare events. *Annu. Rev. Phys. Chem.* **61**, 391–420 (2010).
48. Peters, B., Beckham, G. T. & Trout, B. L. Extensions to the likelihood maximization approach for finding reaction coordinates. *J. Chem. Phys.* **127**, 034109 (2007).
49. Tiwary, P. & Berne, B. Spectral gap optimization of order parameters for sampling complex molecular systems. *Proc. Natl Acad. Sci. USA* **113**, 2839–2844 (2016).
50. M Sultan, M. & Pande, V. S. tICA-metadynamics: accelerating metadynamics by using kinetically selected collective variables. *J. Chem. Theory Comput.* **13**, 2440–2447 (2017).
51. McCarty, J. & Parrinello, M. A variational conformational dynamics approach to the selection of collective variables in metadynamics. *J. Chem. Phys.* **147**, 204109 (2017).
52. Piccini, G., Polino, D. & Parrinello, M. Identifying slow molecular motions in complex chemical reactions. *J. Phys. Chem. Lett.* **8**, 4197–4200 (2017).
53. Chen, W. & Ferguson, A. L. Molecular enhanced sampling with autoencoders: on-the-fly collective variable discovery and accelerated free energy landscape exploration. *J. Comput. Chem.* **39**, 2079–2102 (2018).
54. Wehmeyer, C. & Noé, F. Time-lagged autoencoders: deep learning of slow collective variables for molecular kinetics. *J. Chem. Phys.* **148**, 241703 (2018).
55. Wang, Y., Ribeiro, J. M. L. & Tiwary, P. Past–future information bottleneck for sampling molecular reaction coordinate simultaneously with thermodynamics and kinetics. *Nat. Commun.* **10**, 3573 (2019).
56. Tribello, G. A., Bonomi, M., Branduardi, D., Camilloni, C. & Bussi, G. PLUMED2: new feathers for an old bird. *Comput. Phys. Comm.* **185**, 604–613 (2014).
57. Fiorin, G., Klein, M. L. & Hénin, J. Using collective variables to drive molecular dynamics simulations. *Mol. Phys.* **111**, 3345–3362 (2013).
58. Sidky, H. et al. SSAGES: software suite for advanced general ensemble simulations. *J. Chem. Phys.* **148**, 044104 (2018).
59. Grubmüller, H., Heymann, B. & Tavan, P. Ligand binding: molecular mechanics calculation of the streptavidin-biotin rupture force. *Science* **271**, 997–999 (1996).
60. The PLUMED consortium. Promoting transparency and reproducibility in enhanced molecular simulations. *Nat. Methods* **16**, 670–673 (2019).
61. Dama, J., Rotskoff, G., Parrinello, M. & Voth, G. Transition-tempered metadynamics: robust, convergent metadynamics via on-the-fly transition barrier estimation. *J. Chem. Theory Comput.* **10**, 3626–3633 (2014).
62. Jourdain, B., Lelièvre, T. & Zitt, P.-A. Convergence of metadynamics: discussion of the adiabatic hypothesis. Preprint at [arXiv:https://arxiv.org/abs/1904.08667](https://arxiv.org/abs/1904.08667) (2019).
63. Cuendet, M. & Tuckerman, M. Free energy reconstruction from metadynamics or adiabatic free energy dynamics simulations. *J. Chem. Theory Comput.* **10**, 2975–2986 (2014).
64. Mones, L., Bernstein, N. & Csányi, G. Exploration, sampling, and reconstruction of free energy surfaces with Gaussian process regression. *J. Chem. Theory Comput.* **12**, 5100–5110 (2016).
65. Bussi, G., Gervasio, F. L., Laio, A. & Parrinello, M. Free-energy landscape for beta hairpin folding from combined parallel tempering and metadynamics. *J. Am. Chem. Soc.* **128**, 13435–13441 (2006).
66. Camilloni, C., Provasi, D., Tiana, G. & Broglia, R. A. Exploring the protein G helix free-energy surface by solute tempering metadynamics. *Proteins* **71**, 1647–1654 (2008).
67. McGovern, M. & De Pablo, J. A boundary correction algorithm for metadynamics in multiple dimensions. *J. Chem. Phys.* **140**, 229901 (2013).
68. Harvey, M. J., Giupponi, G. & Fabritiis, G. D. ACEMD: accelerating biomolecular dynamics in the microsecond time scale. *J. Chem. Theory Comput.* **5**, 1632–1639 (2009).
69. Case, D. A. et al. The Amber biomolecular simulation programs. *J. Comput. Chem.* **26**, 1668–1688 (2005).
70. Hutter, J., Iannuzzi, M., Schiffmann, F. & VandeVondele, J. CP2K: atomistic simulations of condensed matter systems. *Wiley Interdiscip. Rev. Comput. Mol. Sci.* **4**, 15–25 (2014).
71. Todorov, I. T., Smith, W., Trachenko, K. & Dove, M. T. DL\_poly\_3: new dimensions in molecular dynamics simulations via massive parallelism. *J. Mater. Chem.* **16**, 1911–1918 (2006).
72. Bowers, K. J. et al. Scalable algorithms for molecular dynamics simulations on commodity clusters. in *Proc. 2006 ACM/IEEE Conf. Supercomput.* 43–43 (IEEE, 2006).
73. Abraham, M. J. et al. GROMACS: high performance molecular simulations through multi-level parallelism from laptops to supercomputers. *SoftwareX* **1**, 19–25 (2015).
74. Kapil, V. et al. i-PI 2.0: a universal force engine for advanced molecular simulations. *Comput. Phys. Commun.* **236**, 214–223 (2019).
75. Anderson, J. A., Lorenz, C. D. & Travesset, A. General purpose molecular dynamics simulations fully implemented on graphics processing units. *J. Comput. Phys.* **227**, 5342–5359 (2008).
76. Plimpton, S. Fast parallel algorithms for short-range molecular dynamics. *J. Comput. Phys.* **117**, 1–19 (1995).
77. Phillips, J. C. et al. Scalable molecular dynamics with NAMD. *J. Comput. Chem.* **26**, 1781–1802 (2005).
78. Loudon, P. et al. OPENMD 2.5: molecular dynamics in the open. *OpenMD* <http://openmd.org/> (2017).
79. Eastman, P. et al. OpenMM 7: rapid development of high performance algorithms for molecular dynamics. *PLoS Comput. Biol.* **13**, e1005659 (2017).
80. Procacci, P. Hybrid MPI/OpenMP implementation of the ORAC molecular dynamics program for generalized ensemble and fast switching alchemical simulations. *J. Chem. Inf. Model.* **56**, 1117–1121 (2016).
81. Tuckerman, M. E., Yarne, D., Samuelson, S. O., Hughes, A. L. & Martyna, G. J. Exploiting multiple levels of parallelism in molecular dynamics based calculations via modern techniques and software paradigms on distributed memory computers. *Comput. Phys. Commun.* **128**, 353–376 (2000).
82. Giannozzi, P. et al. QUANTUM ESPRESSO: a modular and open-source software project for quantum simulations of materials. *J. Phys. Condens. Matter* **21**, 395502 (2009).
83. Gygi, F. Architecture of Qbox: a scalable first-principles molecular dynamics code. *IBM J. Res. Dev.* **52**, 137–144 (2008).

**Author contributions**

Both authors contributed to all aspects of manuscript preparation, revision and editing.

**Competing interests**

The authors declare no competing interests.

**Peer review information**

*Nature Reviews Physics* thanks the anonymous reviewer(s) for their contribution to the peer review of this work.

**Publisher's note**

*Springer Nature* remains neutral with regard to jurisdictional claims in published maps and institutional affiliations.

**Supplementary information**

Supplementary information is available for this paper at <https://doi.org/10.1038/s42254-020-0153-0>.

© Springer Nature Limited 2020